Title

Head response and cervical spine injuries in an oblique lateral helmeted head impact

Authors' information and order

Order	First Name	Family Name	Affiliation(s)
1	Marie-Hélène	Beauséjour	-École de technologie supérieure (Department of Systems Engineering), Montréal (Québec), Canada -Université Gustave Eiffel, Laboratoire de Biomécanique Appliquée, Marseille, France
2	Nicolas	Bailly	Université Gustave Eiffel, Laboratoire de Biomécanique Appliquée, Marseille, France
3	Wei	Wei	Université Gustave Eiffel, Laboratoire de Biomécanique Appliquée, Marseille, France
4	Lucas	Troude	North University Hospital, APHM-AMU (Department of Neurosurgery), Marseille, France
5	Paolo	Panichelli	Université Gustave Eiffel, Laboratoire de Biomécanique Appliquée, Marseille, France
6	Pierre-Jean	Arnoux	Université Gustave Eiffel, Laboratoire de Biomécanique Appliquée, Marseille, France

Corresponding author: Marie-Hélène Beauséjour, marie-helene.beausejour@etsmtl.ca, ORCID: 0000-0001-5720-3712

Statements and Declarations

The authors have no financial interest related to this work. The research protocol was approved by the Laboratoire de biomécanique appliquée under reference PR_Head_Impact. The PMHS were obtained under the reference numbers 32-21, 34-21, 85-21, 108-21 and 106-21 from the Centre de don de corps, Aix-Marseille Université.

Acknowledgments

This study was funded by Gustave Eiffel University. The authors would like to thank Virginie Bascop, Max Py and Camille Bélanger for their technical help as well as Anne Juillet for her help with the results analysis.

Data Availability Declaration

The authors declare that the data supporting the findings of this study are available within the paper and its supplementary information files.

Competing Interest Declaration

The authors have no competing interests to declare.

Abstract

Purpose: Oblique lateral head impacts are common in motorcycle accidents and rollover crashes. However, the neck injury mechanisms following this impact have not been thoroughly described. This work aimed to characterize the head kinematics and cervical spine injuries from oblique lateral helmeted head impacts. Methods: Five post-mortem human surrogates (3 females) were hit laterally on the head with a 37 kg impactor with an oblique plane generating a compressive load. The impact velocities were 4 m/s (3 surrogates) and 5.1 m/s (2 surrogates). The surrogates were equipped with accelerometers on the helmets, in the mouth and at the sternum. Stereography was used to follow the 3D displacements of markers on the helmet. CT-scans and dissection were performed after the impact to assess injuries. Results: The most frequent injuries were posterior ligament ruptures (2 occurrences) and vertebral lamina fractures (2 occurrences). The head maximal accelerations were between 13 and 51 g, and the peak impact forces ranged from 1800 to 5600 N. The head maximal lateral bending was around 30 degrees (4 m/s) or 50 degrees (5.1 m/s). Conclusion: While the measured lateral rotations were under the physiological threshold, they were sufficient to cause injuries at the tested impact energy level. This suggests that the dynamic aspect of the impact and the combination of compression and lateral bending delivered by the oblique impactor are essential in the injury mechanism. This novel data will be determinant in understanding cervical spine injuries and improving the behaviour of human body models.

Keywords: Cervical spine, head impact, trauma, neck injury

INTRODUCTION

Cervical spine injuries can lead to severe conditions, including quadriplegia, and may be sustained from direct head impacts during sports accidents [1,2], motorcycle, cycling, karting, snow sports or vehicle roll-overs [3,4]. Data on direct head impact is scarce, and lateral head impacts, in particular, have been seldom studied while they are common in motorcycle accidents, especially frontal-lateral collisions [5], and in roll-over crashes [3] which are a common cause of death in karting accidents [6]. The mechanism combining axial compression with lateral bending is misknown and has not been reproduced in full human body specimens. There is also no available data on neck injury tolerance to lateral head impact. Injury criteria in all directions are necessary to understand the neck injury response, improve the design of protective equipment like neck braces, and improve automotive safety.

Most previous experimental studies on cervical spine injury have focused on head-first vertex impact [7–11], axial compression [12,13] or sled impacts including lateral sled-tests [14–17]. Volunteers test data were used for the development of anthropometric neck dummies under different directions of loads including lateral loading [18], but additional biomechanical data and injury risk functions are necessary to evaluate the biofidelity of the dummies [19]. Yoganadan et al. [20] submitted whole PMHS and then their isolated head-neck complexes to lateral-flexion moment using an electro-hydraulic test machine, but they used only two specimens, and none were injured. Concerning direct head impacts with a lateral force component, Roberts et al. [3] reproduced roll-over crashes on PMHS and Toomey et al. [4] performed head-neck

specimens drop-tests on an inclined plane. However, the experimental conditions of these two studies do not replicate the conditions of a helmeted head-first impact as seen in motorcycling crashes. The association between helmets and cervical spine injuries is unclear [21], but considering that helmets influence head and neck kinematics [22], experimentally reproducing helmeted head impacts is important to better understand the injury risk in helmeted impact scenarios.

Finite element modeling has been used to gather information on the kinematics of the cervical spine under complex loadings. For example, Barker and Cronin [23] simulated oblique impact on a numerical neck model using kinematics data from volunteer sled test. Neck injury risk curves for lateral sled-impacts were also determined in a previous finite element study using survival analysis from upper and lower neck loads [24]. In both these studies, the authors relied on experimental data to assess the value and credibility of their model. However, these data are scarce or nonexistent for certain impact directions including helmeted oblique lateral head impacts.

No previous experimental study has attempted to reproduce oblique lateral head impacts on PMHS. This experimental study objective was to evaluate head kinematics and cervical spine injuries on human cadavers from a helmeted oblique lateral head impact representative of a motorcycle or karting accident.

MATERIALS AND METHODS

Post-Mortem Human Surrogates

Five PMHS subjects (3 females and 2 males) embalmed with zinc chloride solution (41 %) [25,26] were used in this study. Prior to the test and after the embalmment, PMHS were kept at 6°C. They were between 74 and 91 years old. The weight, height and neck circumference of the subjects are given in Table 1. The PMHS were imaged by computed tomography before the impact to check for spinal anomalies and the C0-T1 length was measured using 3D slicer (http://www.slicer.org) (Table 1). Prior to the tests, the PMHS heads were manually mobilized in flexion-extension, axial rotation and lateral bending for 40 cycles in each direction to precondition the neck tissues. The PMHS were equipped with a medium size Aero helmet (model E11 050023/P-806428 Model FF311) to replicate typical motorcycle or karting roll-overs conditions.

Impact Conditions

The impact conditions are summarized in Table 1. The head impacts were performed by a horizontal impactor (37 kg) propelled by a system of springs. This mass corresponds to the mass of the head, neck, thorax and arms of a 50^{th} percentile male [27] and represents an estimation of the load submitted to the head and neck when a motorcyclist is ejected or during a karting roll-over. Preliminary multi-body simulations of karting roll-over demonstrated the accuracy of the chosen impactor mass. The impactor end was a square of 60 by 60 mm. An oblique plane (45 degrees to the horizontal plane) was designed and added to the impactor (Fig. 1). Oblique impacts

resulting in an important tangential load component are frequent in motorcycle accidents [5,28] and are replicated in helmet testing [29,30].

[Figure 1 approximate placement]

Two impact zones were chosen: a purely lateral impact and a frontal-lateral impact where the impact was rotated by 45 degrees in the axial plane. Both impacts were done on the parietal region at the ¼ superior part of the helmet height (Fig. 1) as proposed by helmet testing protocols [5,29,31]. Both impact zones are expected to result in different neck kinematics. The impact velocities were chosen to match standard helmet testing velocities of 4.5 and 5.5 m/s [29] and previous direct head impact experimentation [32]. The stroke of the impactor was limited to 10 cm after its initial contact with the helmet to ensure full neck lateral bending and to not push the head excessively after the initial contact. The actual experimental stroke was then measured on the videos (Table 1). The test bench design has been described in a previous study [32]. In brief, the test bench is made from an isolated car seat and rails fixed onto an elevation table. The subjects were seated and immobilized with three straps: one under the armpits, one at the hip and one at the chest and over the arms (Fig. 1). A soft plastic device was positioned behind the neck of the subject to maintain the head and neck in a neutral posture before the impact.

[Table 1 approximate placement]

Instrumentation

The PMHS were equipped with sets of three linear accelerometers (capacity of ±250 g, EGAS S403A-250- /L1.5M, TE Connectivity, Schaffhouse, Switzerland) at the sternum, in the mouth and the top of the helmet. At the sternum, the accelerometer was screwed into the bone, at the helmet, the accelerometer was glued with heavy duty contact glue and, in the mouth, the accelerometer was put in placed and fixed using spray rigidifying foam. A load cell was placed on the impactor (capacity of ±30 kN, type 9347C, Kistler, Winterthur, Switzerland). The accelerometers and the load cell recorded at 10,000 Hz. Markers were fixed on the surrogates' helmets to measure the head 3D kinematics by stereography (Fig. 1). The impacts were filmed at 1,000 Hz by two high speed cameras (Fastcam SA3, Photron, San Diego, United States). The software Vic3D (Correlated Solutions, Irmo, United States) was used for the markers tracking.

Data Analysis

The accelerometers and force data were filtered with a low-pass second-order Butterworth filter (cut-off frequency of 1,000 Hz) as recommended by the SAE J211 specifications. The resultant of the mouth accelerations was reported. The helmet rotation and translation during the impact were measured by using the set of markers placed on top of the helmet (Fig. 1). The rotation matrix (**R**) of these points was measured throughout the test using the Kabsch algorithm [33] and using the position prior to the impact as the reference point. The rotations were measured from **R** using

the roll, law and pitch method using the following equations where **R** is the rotation matrix and **i** is the time step.

Axial rotation (yaw):

$$yaw(i) = \frac{180}{\pi} atan^2(\boldsymbol{R}(2,1,i), \boldsymbol{R}(1,1,i))$$

Flexion-Extension (pitch):

$$pitch(i) = \frac{180}{\pi} atan^2(\boldsymbol{R}(3,1,i), \sqrt{(\boldsymbol{R}(3,2,i)^2 + \boldsymbol{R}(3,3,i)^2)})$$

Lateral bending (roll)

$$roll(i) = \frac{180}{\pi} atan^2(\boldsymbol{R}(3,2,i), \boldsymbol{R}(3,3,i))$$

Injury Analysis

The PMHS were imaged by computed tomography (CT) before and after the impact. The images were reviewed by a neurosurgeon to check for bone fracture or spine dealignment. The cervical spines were also dissected by a neurosurgeon after the impact to assess potential soft tissue injuries. Pre- and post-impact flexibility test was performed to assess potential cervical spine instability, which may not be visible on the CT scans or during autopsy. The head of each PMHS was mobilized manually in flexion-extension, axial rotation and lateral bending without a helmet until a significant resistance was felt by the experimenter [32]. This significant resistance was subjectively identified by the experimenter to approximate the head range of motion. Four markers were glued on the PMHS mask to trace a cranial-caudal vector and right-left vector. The

mobilization was filmed and Vic3D was used to follow the markers. The head rotation was calculated as the Euler angle between the initial vector (resting position) and the current vector at each time step. The maximal rotation in all the directions was then calculated before and after the impact. Finally, the peak resultant mouth acceleration and the peak resultant impact force was plotted in function of the injuries severity. The severity of the injuries was graded following the AO classification with A types injuries being less severe than type B and type B less severe than type F [34].

RESULTS

The injuries found for all PMHS are detailed in Table 2 and Fig. 2 and an AO classification is give for each injury [34]. Amongst the five surrogates, two had no sign of injury on the CT-scan images or at the autopsy. Lamina fractures (AO classification A0) were seen on two subjects at C3 or C7. One case of articular facet fracture was found at C4-C5 in the contralateral side of the impact and one case of C1 lateral mass fracture occurred at the ipsilateral side of the impact (AO classification F1). Posterior ligaments ruptures at the subaxial cervical spine (AO classification B2) were seen on two subjects at C1-C2 and C2-C3 (PMHS 1) and C5-C6 (PMHS 4).

[Table 2 approximate placement]

[Figure 2 approximate placement]

The post-prior impact differences in range of motion are presented in Fig. 3. The difference was generally higher in lateral bending as expected, but axial rotation was also affected. The subjects with no sign of injury (PMHS 3 and 5) had minimal differences in range of motion.

151 [Figure 3 approximate placement]

152 The results from the impact load cell are presented in Fig. 4. The maximum
153 resultant force was between 1,800 N (PMHS 2) and 5,600 N (PMHS 4). For all cases, the
154 force normal to the impactor (Z) was the highest. The force pattern presents two local
155 maximums for all PMHS except PMHS 4 which is typical for helmet impact absorption.
156 Increasing the velocity of the impact increased the impact force.

157 [Figure 4 approximate placement]

158 The resultant accelerations measured from the linear accelerometers place
159 inside the surrogates' mouth are presented in Fig. 5. The resultant peak acceleration is
160 between 13 (PMHS 2) and 51 g (PMHS 3). Increasing the impactor velocity generally
161 increased the mouth acceleration.

162 [Figure 5 approximate placement]

163 The sternum resultant acceleration was under 7 g for PMHS 2, 3 and 4 while it
164 reached 73 g for PMHS 1 (Table 3). The amplitude of this acceleration could be
165 explained by the contact of the helmet on the shoulder or clavicle. In all cases, the
166 maximum resultant sternum acceleration occurred after the helmet-impactor contact
167 and after the maximum mouth acceleration. The sternum and helmet acceleration data
168 for each PMHS are available in **Online Ressource**.

169 [Table 3 approximate placement]

170 The helmet 3D range of motions is presented in Fig. 6. As expected, lateral
171 bending was the most important motion and flexion-extension was limited. Lateral
172 bending was accompanied by axial rotation (around 10 degrees), which is normal

considering the anatomy of the cervical spine and the 3D orientation of the articular facets. As expected, increasing the velocity of impact from 4 to 5.1 m/s increased the lateral range of motion from approximately 30 degrees to about 50 degrees.

[Figure 6 approximate placement]

The helmet 3D translations are presented in Fig. 7. Increasing the velocity of impact (from 4 to 5.1 m/s) increased the lateral translation as expected: from around 200 mm to 300 mm. Data are missing at the peak of motion for PMHS 3 and 5 because the markers exited the field of view of the cameras.

[Figure 7 approximate placement]

The relationship between the severity of the injuries and the head acceleration or the impact force represented in Fig. 8 did not yield any particular pattern.

[Figure 8 approximate placement]

DISCUSSION

This study conducted direct lateral head impacts with an oblique impactor on five helmeted PMHS and collected unique data on head kinematics and the resulting cervical spine injuries. Very few studies reproduced lateral neck injuries on full-scale subjects as can be noted from Booth et al. [35] review. Therefore, these experimental tests provide new data to understand dynamic head impact and lateral neck loadings and to establish relevant lateral neck injury criteria. Future studies could use these data to validate finite element models which could then be used to further our knowledge of spinal injuries or to test protective devices.

195 The accelerations and forces measured were consistent within the tests
196 performed at the same velocity (4 or 5.1 m/s). The mouth accelerations (13 – 51 g) and
197 the resultant impact loads (1,800 – 5,600 N) increased with the speed of the impact.
198 Compared to a previous study on rear-head impact performed at similar velocities [32],
199 the resultant accelerations in this study were smaller probably due to the neck higher
200 rigidity in lateral bending [36]. The impact loads were higher for the oblique lateral tests
201 than for rear-head impact on PMHS: 1,800 – 2,700 N [32]. Melnyk et al. [37] performed
202 compressive loads at various lateral eccentricity on specimens of two functional spinal
203 units and obtained compressive loads between 699 N and 6,207 N which is similar to
204 our results even though the loading conditions are quite different. Hybrid III dummy
205 drop-tests reproducing a helmeted cyclist ejection accident measured an upper neck
206 force of approximately 2,000 N in compression and 450 N in shear for a lateral impact at
207 2.48 to 2.65 m/s [38] which is similar to the loads we obtained at the impactor for
208 similar velocities.
209 The most frequent injuries detected here were: rupture of the posterior
210 ligaments and fracture of the lamina. These injuries were consistent with previous
211 results on car rollovers that produced mostly unilateral soft tissues injuries [3]. The
212 lamina fractures were also consistent the observations of Whyte et al., [39] who
213 performed a series of experiments on functional spinal units under anterior, posterior
214 and lateral shear forces and reported contact between the articular facet and the
215 lamina at the intervertebral level for functional spinal units submitted to lateral shear
216 and compression. Fracture of the lamina was also frequently reported in an

217 experimental study performing inverted head-neck specimens drop on an 15 degrees
218 inclined surface at 2.91 - 3.26 m/s [4]. In the present study, only one PMHS was
219 subjected to the frontal-lateral impact (case 5), but while the measured impact loads
220 were higher than for cases 1 and 2 performed at the same velocity, no injury was
221 detected. This may be due to the higher flexibility of the cervical spine in extension
222 compared to lateral bending.

223 Interestingly, PMHS 4 experienced high head acceleration and impact force, but
224 did not sustain any visible injury, while PMHS 1 and 2, which experienced the lowest
225 impact forces and head accelerations, sustained vertebral fractures. This is likely due to
226 variability between subjects. For instance, PMHS 1 and 2 were both females weighing
227 approximately 65 kg, whereas PMHS 4 was a male weighing 78 kg. Indeed, females are
228 less resistant to compressive injuries [39]. These results illustrate that interindividual
229 differences (sex, age, height, weight) have an important influence on injury vulnerability
230 and emphasize the need to account for individual parameters in the development of
231 injury criteria. Future studies combining numerical modeling and experimentations
232 should be done to investigate further the relationship between impact metrics, for
233 example head acceleration, and injuries.

234 Previous studies on compressive loading combined with lateral eccentricity
235 performed on functional spinal units reported that low eccentricity results in hard tissue
236 injury, while higher eccentricity leads to more soft tissue injury including intervertebral
237 disc and ligament injuries [37,39]. In this study, while the number of specimens is
238 limited, we observed a roughly equal number of soft and hard tissue injuries.

239 Considering the typology of the obtained fractures, they result from the lateral and
240 compressive loads applied to the spine.
241 Neck range of motion was measured before and after the impact as post-
242 traumatic range of motion is an important indicator of cervical spine injuries. While it
243 was measured manually, which does not allow the operator to control the applied loads
244 and is subjective, the results showed higher differences in range of motion for subjects
245 with ligamentous injuries, which is consistent with clinical observations [40]. The PMHS
246 with no sign of injuries showed little to no increase of range of motion which suggests
247 that the PMHS were indeed not injured. Both the lateral and axial rotation range of
248 motion were increased after the impact, for PMHS 1 and 3, showing the posterior
249 ligaments contribution to both motions.
250 The normal force (Fz) was always greater than the tangential force (Fy) with a
251 ratio of 1/9 to 1/2. The head maximum translation was negligible in the antero-posterior
252 and cranial-caudal directions and reached 200 – 300 mm in the lateral direction. PMHS 4
253 experienced the highest lateral translation but did not show any sign of injury. Since this
254 subject had the highest C0-T1 length, it points out that these values should be put in
255 relation to the individual morphology. However, data on injury threshold for translation
256 is missing, while it would be useful to better understand the injury mechanism. The
257 average neck lateral bending measured on healthy volunteers wearing a helmet is
258 between 37±8.7 degrees (right) or 41.8±6.6 degrees (left) [33], while the peak lateral
259 bending reached 50 degrees during the impact. Therefore, the measured peak lateral
260 bending in this study was within the physiological range showing that lateral bending

alone is not responsible for the injuries. Head lateral bending was combined with axial rotation similarly to Barker and Cronin [23] in their oblique sled-impact simulations who reported a combination of head forward excursion, lateral bending and axial rotation during the impact, but the axial rotation was limited to 10-20 degrees. Since the cervical spine range of motion is within physiological value, the impact compressive component appears to be essential in the injury mechanism.

As with any experimental work, this study presents limitations. First, this study was performed with PMHS wearing a helmet, which influences the kinematics and injury response and limits its transferability to unhelmeted head impact. The PMHS were between 74 and 91 years old, while high-energy traumatic spine injuries occur more frequently to younger individuals [41]. Aging leads to degeneration of the tissues and stiffening of the cervical spine [42] which affects its response to injury. Still, the number of elderly worldwide is increasing and it is important to improve our knowledge of how the elderly spine behaves in traumatic conditions. The embalmment process may lead to changes in the tissue mechanics that have not been thoroughly studied due to the newness of the Zinc Chloride usage. However, the muscles remain subjectively flexible [25]. While muscle activation is important to hold the head and neck posture while wearing a helmet, it was not present in this experiment. Muscle activation, which has been reported at 50 to 100 ms after impact, also influences head kinematics by limiting head displacement [23]. However, for high-velocity head impact, the effect of the osteoligamentous structures are more important [43]. The surrogates were strapped to the seat to limit torso motion and isolate neck motion. As a result, the torso boundary

283 conditions may differ from those in motorcycle or karting crashes, where the torso is
284 not restrained. Pre- and post-flexibility testing was performed manually. The results are
285 therefore subjective to the experimenter and should be treated as an approximation of
286 the PMHS head range of motion.

287 The number of surrogates was limited as is often the case with cadaveric studies,
288 but finite element modeling could be used to generate more data. Simulation could also
289 be used to investigate the biofidelity of the obtained neck responses since similar
290 experiments are absent in the literature. The sensors and video analysis enabled us to
291 follow the helmet and head motion, but the intervertebral displacement is left unseen.
292 Future tests using fluoroscopy to visualize the cervical spine movement should be
293 performed to distinguish how the applied impact is distributed along the spine and
294 identify injury mechanisms like spine buckling or intervertebral shearing. To compare
295 the results to injury thresholds, for example the eccentricity criteria developed by
296 Whyte et al. [39], it appears interesting to use finite element modeling to measure how
297 the global impact relates to loads and displacements at the intervertebral level.

298 To conclude, the present study reports the head kinematics and cervical spine
299 injuries for five PMHS following oblique lateral and frontal-lateral impacts, which are
300 impact scenarios that have seldom been reproduced experimentally. The impact loads
301 were between 1,800 N and 5,600 N, and the mouth peak acceleration was between 13
302 and 51 g. The head kinematics demonstrate that oblique lateral head impact is
303 accompanied by head axial rotation (approximately 10 degrees). The maximum lateral
304 bending was around 30 degrees for impact at 4 m/s and around 50 degrees for impacts

at 5.1 m/s. Cervical spine injuries were present even for lateral bending within physiological threshold, demonstrating that injuries can occur even for low lateral rotation. The normal loads were two to nine times higher than the tangential loads, which suggests that the compression mechanism is determinant in the injury occurrence. To conclude, the results are of significant value to understand cervical spine injury mechanisms and to validate and develop finite element models to support design and new evaluation procedures for safety devices.

REFERENCES

1. Bailly N, Llari M, Donnadieu T, Masson C, Arnoux P-J. Numerical Reconstruction of Traumatic Brain Injury in Skiing and Snowboarding. Med Sci Sports Exerc [Internet]. 2018;50. Disponible sur: https://journals.lww.com/acsm-msse/fulltext/2018/11000/numerical_reconstruction_of_traumatic_brain_injury.17.aspx

2. Le Flao E, Siegmund GP, Borotkanics R. Head Impact Research Using Inertial Sensors in Sport: A Systematic Review of Methods, Demographics, and Factors Contributing to Exposure. Sports Med. 2022;52:481-504.

3. Roberts CW, Toczyski J, Kerrigan JR. Cervical spine injury in rollover crashes: anthropometry, excursion, roof deformation, and ATD prediction. Clin Biomech. 2019;64:42-8.

4. Toomey DE, Mason MJ, Hardy WN, Yang KH, Kopacz JM, Van Ee C. Exploring the role of lateral bending postures and asymmetric loading on cervical spine compression responses. 2009. p. 375-82.

5. Nicolas B, Sounak M, Piantini S, Caroline D, Pierini M, Willinger R. Proposal of a new motorcycle helmet test method for tangential impact. IRCOBI-Int Res Counc Biomech Inj. IRCOBI; 2016. p. 479-89.

6. Adler P. Go-kart/Fun-kart related injuries and deaths, 1985-1996 [Internet]. Consumer Product Safety Commission; 1998. Disponible sur: https://www.cpsc.gov/s3fs-public/pdfs/gokart.pdf

7. Ivancic PC. Head-first impact with head protrusion causes noncontiguous injuries of the cadaveric cervical spine. Clin J Sport Med. 2012;22:390-6.

8. Saari A, Itshayek E, Cripton PA. Cervical spinal cord deformation during simulated head-first impact injuries. J Biomech. 2011;44:2565-71.

9. Nightingale RW, McElhaney JH, Richardson WJ, Myers BS. Dynamic responses of the head and cervical spine to axial impact loading. J Biomech. 1996;29:307-18.

10. Nightingale RW, McElhaney JH, Richardson WJ, Best TM, Myers BS. Experimental impact injury to the cervical spine: relating motion of the head and the mechanism of injury. JBJS. 1996;78:412-21.

11. Nightingale RW, Richardson WJ, Myers BS. The effects of padded surfaces on the risk for cervical spine injury. Spine. 1997;22:2380-7.

12. Maiman DJ, Yoganandan N, Pintar FA. Preinjury cervical alignment affecting spinal trauma. J Neurosurg Spine [Internet]. 2002;97. Disponible sur: https://thejns.org/spine/view/journals/j-neurosurg-spine/97/1/article-p57.xml

13. Maiman DJ, Sances A Jr, Myklebust JB, Larson SJ, Houterman C, El-Ghatit AZ. Compression Injuries of the Cervical Spine: A Biomechanical Analysis. Neurosurgery. 1983;13:254-60.

14. Lopez-Valdes FJ, Lau A, Lamp J, Riley P, Lessley DJ, Damon A, et al. Analysis of spinal motion and loads during frontal impacts. Comparison between PMHS and ATD. Association for the Advancement of Automotive Medicine; 2010. p. 61.

15. Meyer F, Humm J, Purushothaman Y, Willinger R, Pintar FA, Yoganandan N. Forces and moments in cervical spinal column segments in frontal impacts using finite element modeling and human cadaver tests. J Mech Behav Biomed Mater. 2019;90:681-8.

16. Ewing C, Thomas D, Lustik L, Muzzy W, Willems G, Majewski P. Dynamic response of the human head and neck to+ Gy impact acceleration. SAE Technical Paper; 1977. Report No.: 0148-7191.

17. Ewing C, Thomas DJ, Beeler GW, Patrick LM, Gillis DB. Dynamic Response of the Head and Neck of the Living Human to—G x Impact Acceleration. SAE Technical Paper; 1968. Report No.: 0148-7191.

18. Wang ZJ, Loeber BH, Tesny A, Kang YS. Biomechanical Responses of a New Neck for THOR-AV 5th Percentile Female Dummy. Stockh IRCOBI. 2023;

19. Kang Y, Stammen J, Moorhouse K, Bolte IV J. Head and Neck Responses of Post Mortem Human Subjects in Frontal, Oblique, Side and Twist Scenarios. 2018.

20. Yoganandan N, Humm J, Pintar FA, Wolfla CE, Maiman DJ. Lateral neck injury assessments in side impact using post mortem human subject tests. Association for the Advancement of Automotive Medicine; 2011. p. 169.

21. Khor D, Inaba K, Aiolfi A, Delapena S, Benjamin E, Matsushima K, et al. The impact of helmet use on outcomes after a motorcycle crash. Injury. 2017;48:1093-7.

22. Jadischke R, Viano DC, McCarthy J, King AI. The effects of helmet weight on hybrid III head and neck responses by comparing unhelmeted and helmeted impacts. J Biomech Eng. 2016;138:101008.

23. Barker J, Cronin DS. Muscle activation affects kinematic response and injury risk in non-traditional oblique impact scenarios assessed with a head and neck finite element model. SAE Int J Transp Saf. 2022;10.

24. Meyer F, Humm J, Yoganandan N, Leszczynski A, Bourdet N, Deck C, et al. Development of a detailed human neck finite element model and injury risk curves under lateral impact. J Mech Behav Biomed Mater. 2021;116:104318.

25. Goodarzi N, Akbari G, Razeghi Tehrani P. Zinc chloride, a new material for embalming and preservation of the anatomical specimens. Anat Sci J. 2018;15:25-30.

26. Shang S, Masson C, Teeling D, Py M, Ferrand Q, Arnoux P-J, et al. Kinematics and dynamics of pedestrian head ground contact: A cadaver study. Saf Sci. 2020;127:104684.

27. Davis ML, Vavalle NA, Gayzik FS. An evaluation of mass-normalization using 50th and 95th percentile human body finite element models in frontal crash. 2015. p. 608-21.

28. Chinn B, Canaple B, Derler S, Doyle D, Otte D, Schuller E, et al. COST 327 Motorcycle safety helmets. Eur Comm Dir Gen Energy Transp. 2001;3:1135-48.

29. Pang TY, Thai K, McIntosh A, Grzebieta R, Schilter E, Dal Nevo R, et al. Head and neck responses in oblique motorcycle helmet impacts: a novel laboratory test method. Int J Crashworthiness. 2011;16:297-307.

30. Juste-Lorente Ó, Maza M, Piccand M, López-Valdés FJ. The influence of headform/helmet friction on head impact biomechanics in oblique impacts at different tangential velocities. Appl Sci. 2021;11:11318.

31. Ebrahimi I, Golnaraghi F, Wang GG. Factors influencing the oblique impact test of motorcycle helmets. Traffic Inj Prev. 2015;16:404-8.

32. Beauséjour M-H, Petit Y, Wagnac É, Melot A, Troude L, Arnoux P-J. Cervical spine injury response to direct rear head impact. Clin Biomech. 2022;92:105552.

33. Lecoublet B, Boisclair D, Evin M, Wagnac E, Petit Y, Aubin C-E, et al. Assessing the global range of motion of the helmeted head through rotational and translational measurements. Int J Crashworthiness. 2019;

34. Vaccaro AR, Koerner JD, Radcliff KE, Oner FC, Reinhold M, Schnake KJ, et al. AOSpine subaxial cervical spine injury classification system. Eur Spine J. 2016;25:2173-84.

405 35. Booth GR, Cripton PA, Siegmund GP. The lack of sex, age, and anthropometric
406 diversity in neck biomechanical data. Front Bioeng Biotechnol. 2021;700.

407 36. Watier B. Comportement mécanique du rachis cervical: une revue de littérature.
408 Itbm-Rbm. 2006;27:92-106.

409 37. Melnyk A, Whyte T, Thomson V, Marion T, Yamamoto S, Street J, et al. The Effect
410 of Compression Applied Through Constrained Lateral Eccentricity on the Failure
411 Mechanics and Flexibility of the Human Cervical Spine. J Biomech Eng.
412 2020;142:101005.

413 38. Pang TY, Thai K, McIntosh A. Head and neck dynamics in helmeted Hybrid III
414 impacts. International Research Council on the Biomechanics of Impacts Zurich …;
415 2009. p. 9-11.

416 39. Whyte T, Melnyk AD, Van Toen C, Yamamoto S, Street J, Oxland TR, et al. A neck
417 compression injury criterion incorporating lateral eccentricity. Sci Rep. 2020;10:1-13.

418 40. Izzo R, Popolizio T, Balzano RF, Pennelli AM, Simeone A, Muto M. Imaging of
419 cervical spine traumas. Eur J Radiol. 2019;

420 41. Wagnac E, Mac-Thiong J-M, Arnoux P-J, Desrosiers J-M, Ménard A-L, Petit Y.
421 Traumatic spinal cord injuries with fractures in a Québec level I trauma center. Can J
422 Neurol Sci. 2019;46:727-34.

423 42. Yukawa Y, Kato F, Suda K, Yamagata M, Ueta T. Age-related changes in osseous
424 anatomy, alignment, and range of motion of the cervical spine. Part I: Radiographic data
425 from over 1,200 asymptomatic subjects. Eur Spine J. 2012;21:1492-8.

426 43. Kuo C, Sheffels J, Fanton M, Yu IB, Hamalainen R, Camarillo D. Passive cervical
427 spine ligaments provide stability during head impacts. J R Soc Interface.
428 2019;16:20190086.

429

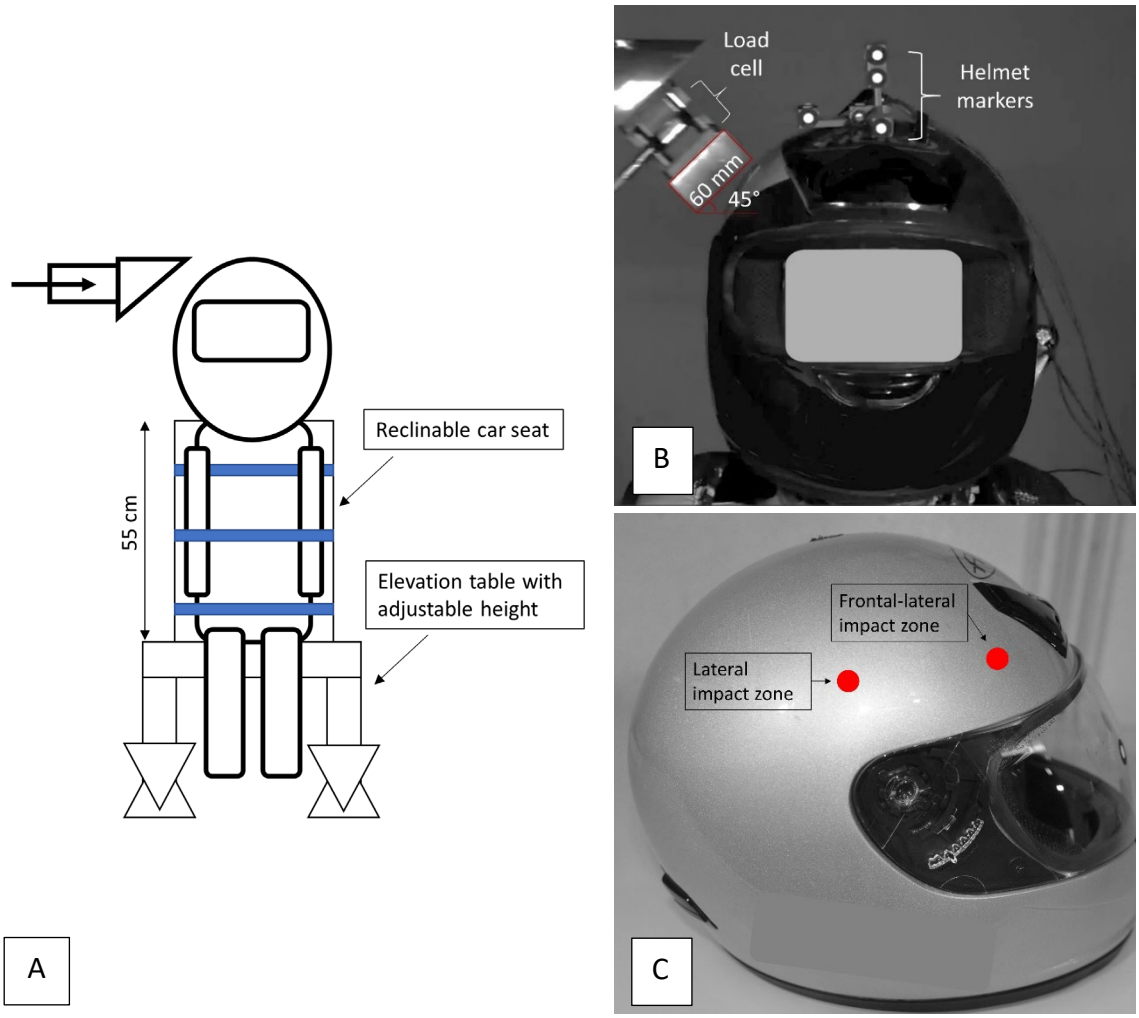

Fig. 1 - Experimental set-up. A) Experimental bench and subject immobilization straps in blue. B) Impactor and markers position. C) Impact zones.

435

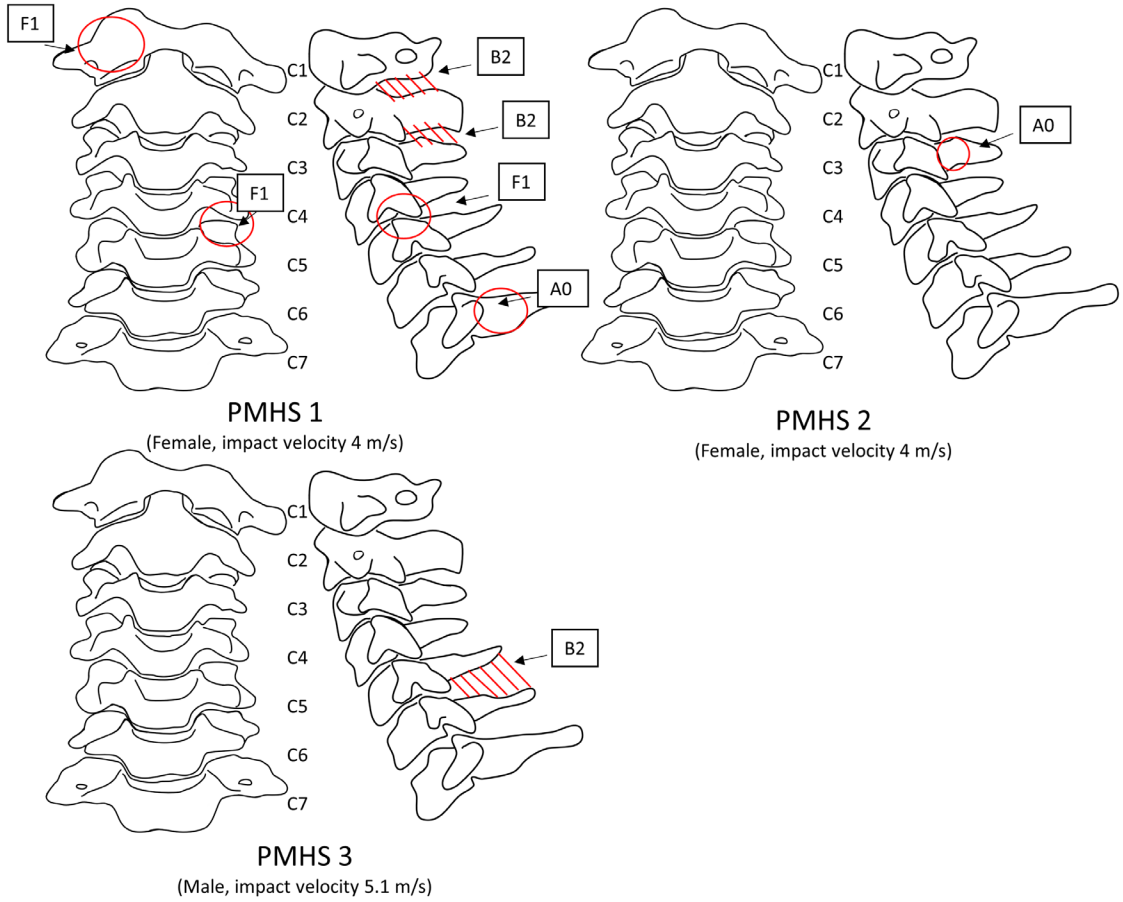

436

437 **Fig. 2** – Schematic representations of the injuries found on the post-mortem human
438 surrogates after impact. Fractures are situated by red circles and ligamentous injuries by
439 red dashes.
440
441

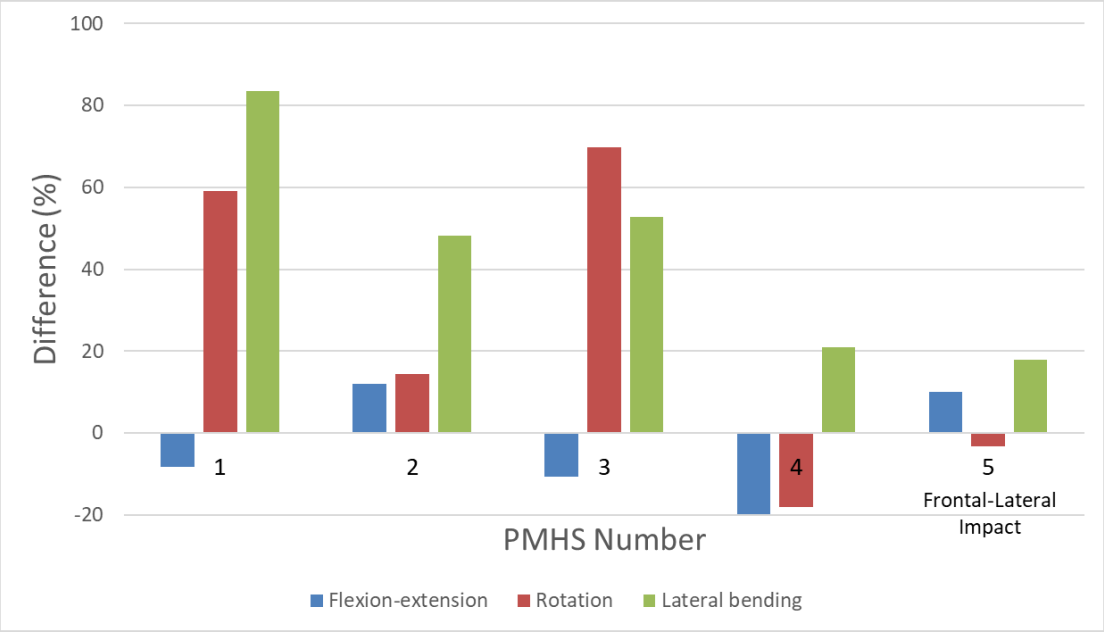

Fig. 3 - Differences in head range of motion measured by manual rotation before and after the impact

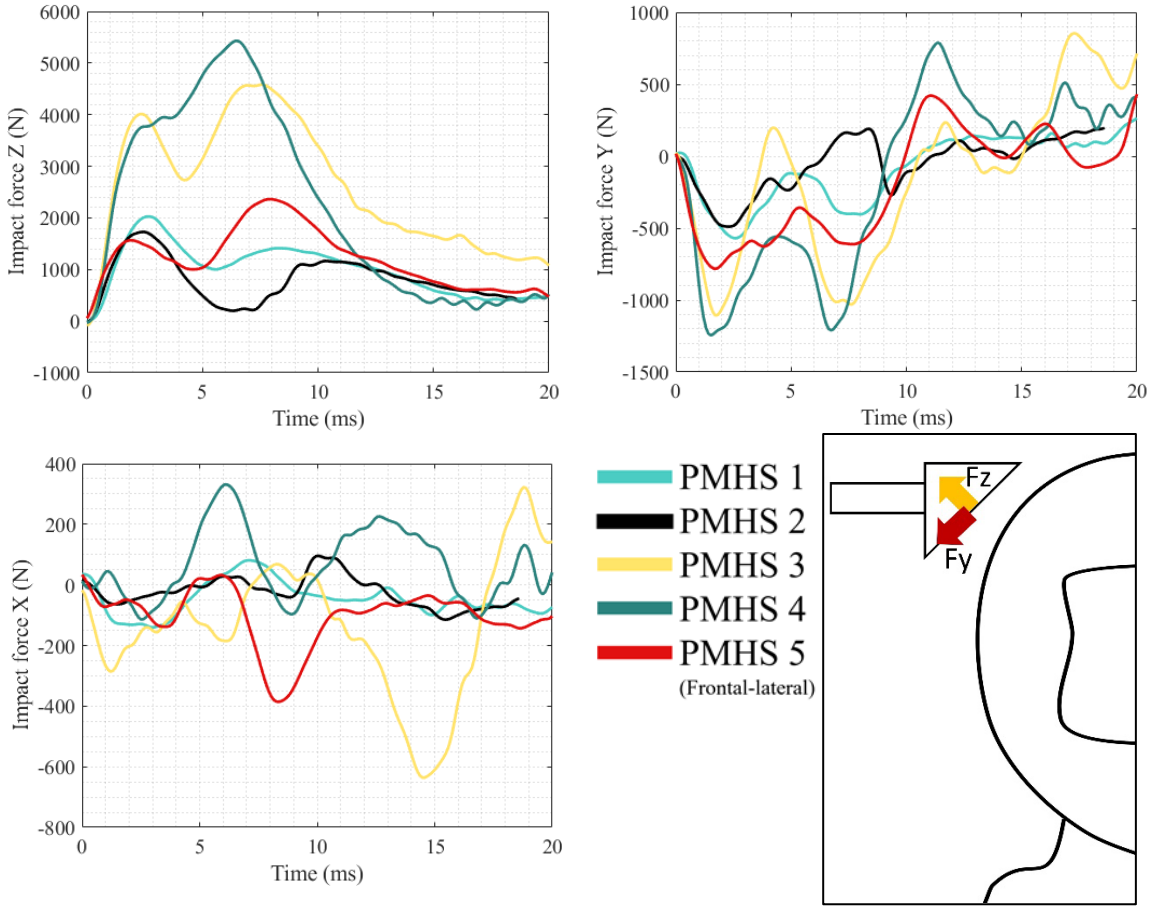

Fig. 4 - Forces measured at the impactor. The Z axis is normal to the impactor and Y is tangential to the impactor

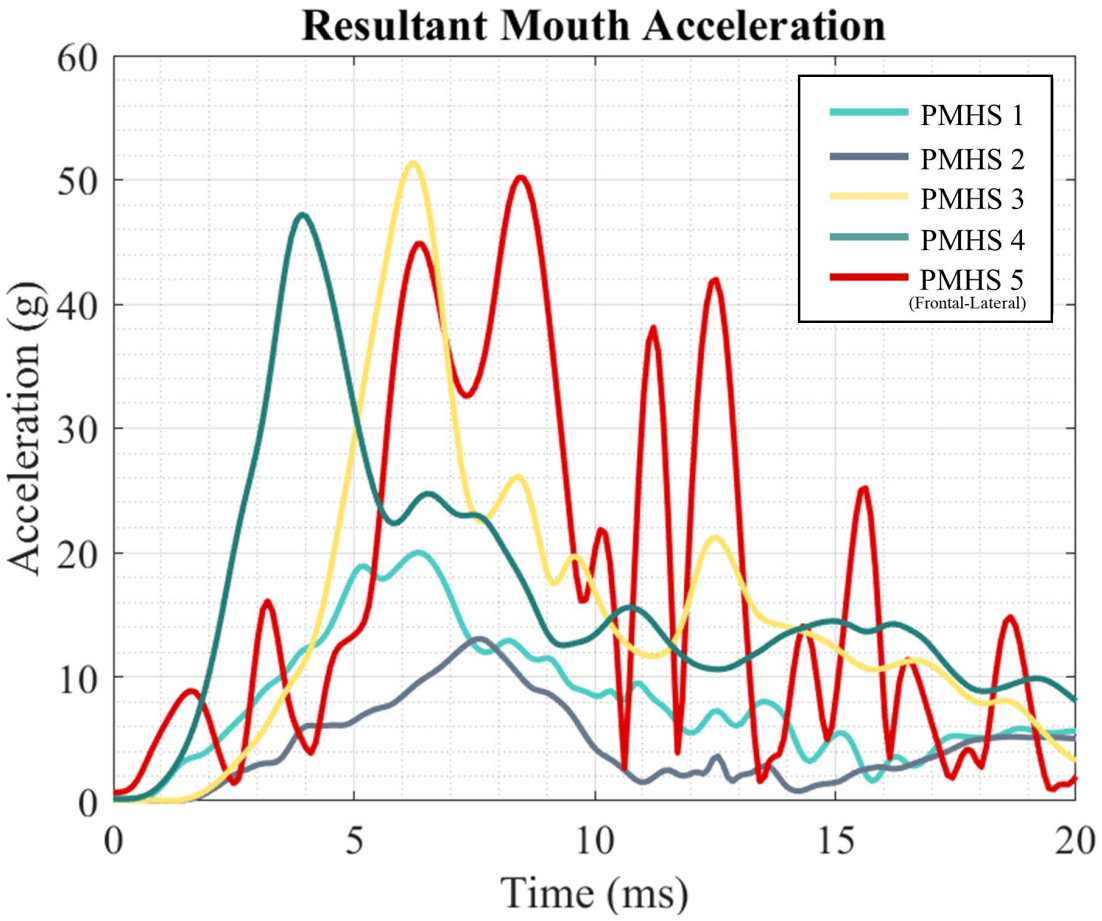

Fig. 5 - Resultant mouth accelerations for each of the post-mortem human surrogates

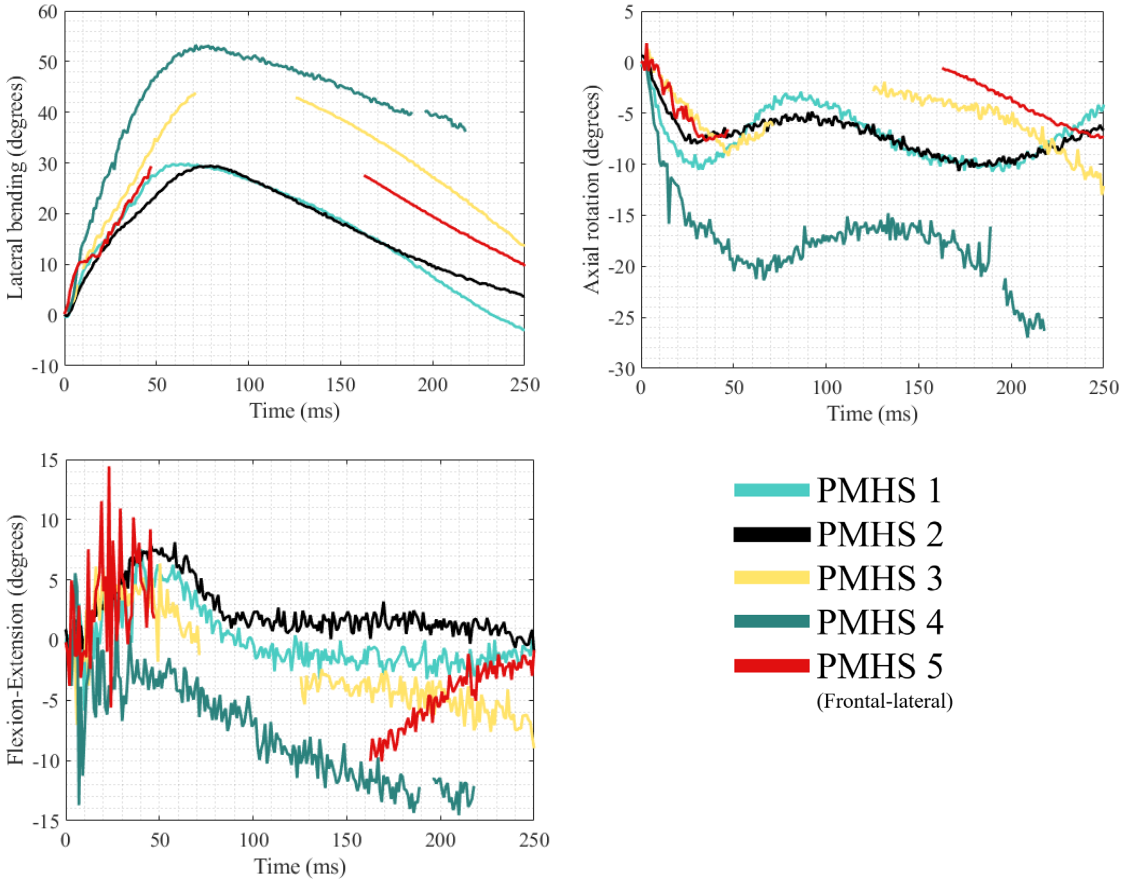

Fig. 6 - Helmet range of motions. Lateral bending is positive towards the left (away from the impactor), flexion is positive and axial rotation is positive towards the left. Data are missing at the apex of the motion for PMHS 3 and 5.

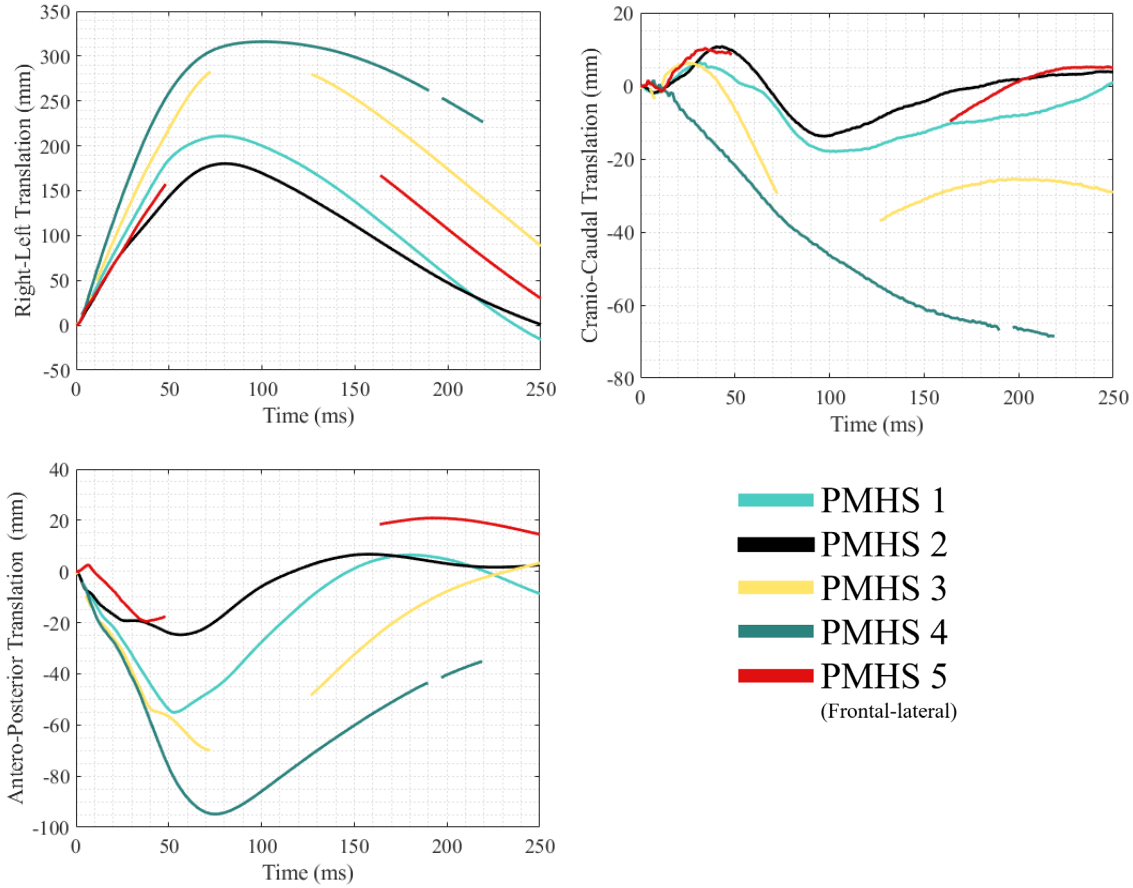

Fig. 7 - Helmet translations for each of the subjects. The right-left translation is positive in the left direction, the antero-posterior translation is positive in the anterior direction and the cranio-caudal translation is positive in the cranial direction. Data are missing at the apex of the motion for PMHS 3 and 5.

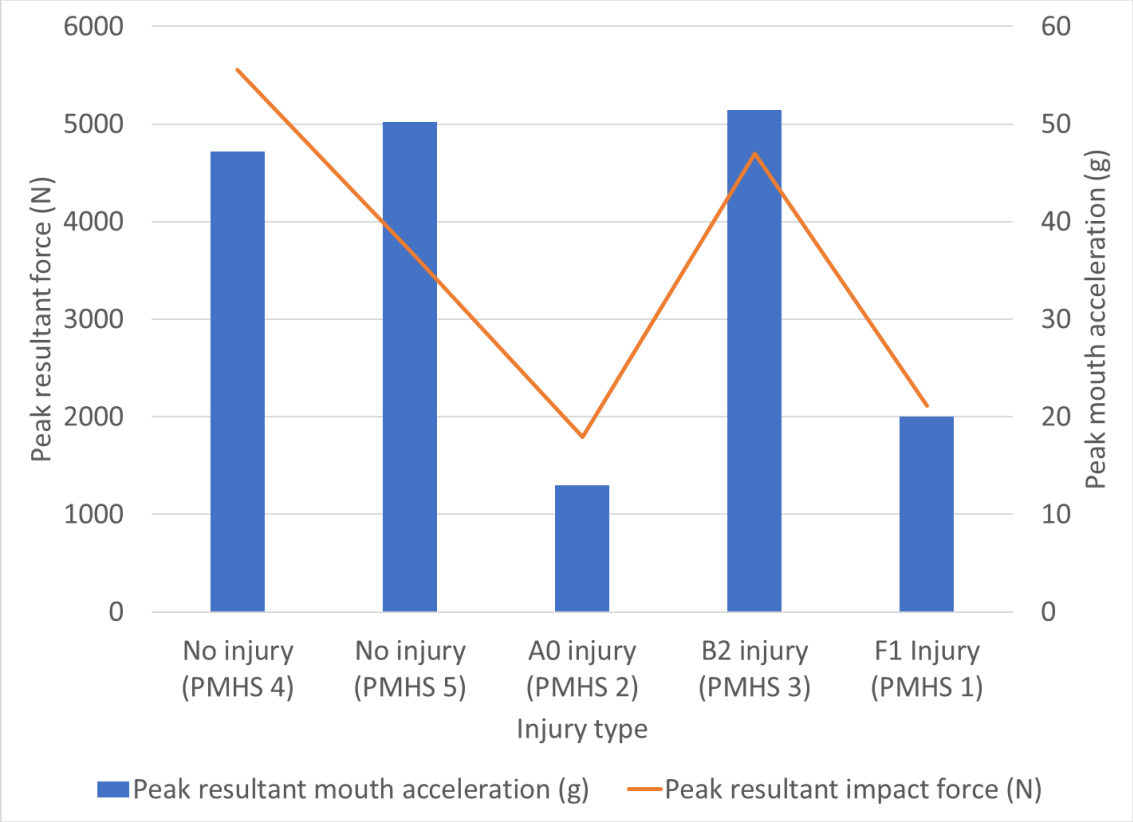

Fig. 8 – Peak resultant force and peak resultant mouth acceleration relative to injury severity. The injuries were placed in increasing severity from left to right following the AO Classification.

474 Table 1 Surrogates' information and impact conditions
475

PMHS number	Impact configuration	Velocity of impact (m/s)	Measured Impact stroke (cm)	Gender	Age	Height (cm)	Weight (kg)	Neck circumference (cm)	Neck Length (C0-T1) (cm)	Trabecular bone mineral density (mg/cc)
1	Lateral	4	16	F	79	161	67	41	12	316
2	Lateral	4	9	F	74	159	64	47	10.8	475
3	Lateral	5.1	16	M	79	172	78	53	11.7	384
4	Lateral	5.1	13	M	91	175	78	46	12.8	212
5	Frontal-lateral	4	10	F	82	154	56	38	10.9	295

476
477

478 Table 2 Surrogates' injury report
479

PMHS number	Injuries found at autopsy	Injuries found on CT-scan images	AO Classification
1	Rupture of posterior ligaments at C1-C2 and C2-C3 Fracture at C4-C5 articular facet (left, opposite side from impact)	Lamina fracture at C7 Fracture of right lateral mass at C1	**F1** (C4-C5) **F1** (C1) **B2** (C1-C2 and C2-C3) **A0** (C7)
2	No visible sign	Lamina fracture at C3	**A0**
3	Rupture of posterior ligaments at C5-C6	No visible sign	**B2**
4	No visible sign	No visible sign	-
5	No visible sign	No visible sign	-

480

481 Table 3 Sternum maximum resultant acceleration
482

PMHS	1	2	3	4	5
Max acceleration (g)	73	3.5	4.4	6.8	ERROR
Time of maximum acceleration (ms)	12.4	12.1	18.4	22.5	ERROR

483
484